Supplemental Discussion:

H3K9me3 and RNAi inheritance. Here we show that HRDE-1, and the downstream nuclear RNAi factors, link dsRNA to H3K9me3 in germline nuclei, and that this HRDE-1 mediated H3K9me3 mark is heritable (Fig. 2d, and Fig. S10). RNAi-directed H3K9me3 is linked to gene silencing in *S. Pombe* (1). In *C. elegans*, RNAi-directed H3K9me3 correlates with RNAi-mediated transcriptional gene silencing (2,3), however, the function of H3K9me3 during *C. elegans* RNAi is not known. During the first generation of RNAi inheritance in *C. elegans*, heritable RNAi silencing depends upon a dominant extra-genic agent that can act independently of the originally RNAi-targeted locus (4,5). These data indicate that (at least in early generations) H3K9me3 cannot be the sole mediator of heritable RNAi silencing.

Despite this, chromatin-modifying and chromatin-associating factors have been linked to long-term RNAi inheritance in *C. elegans* (6). In addition, NRDE-1, which is required for RNAi inheritance, is directed to associate with chromatin by siRNAs (3). The following observation suggests that an RNAi-directed H3K9me3 chromatin marks may contribute to long-term RNAi inheritance in *C. elegans*. Consistent with previous reports (4,5), we found that in early generations of RNAi inheritance gene silencing could act in *trans*: *gfp* RNAi in the parental generation could silence a naïve *gfp* locus in F1 inheriting animals (Fig. S10c). In later generations of RNAi inheritance, however, gene silencing was more pronounced at the allele that had been exposed to *gfp* dsRNA in the parental generation (*cis-restricted*) (Fig. S10c). These data show that (at least in certain cases) RNAi inheritance can be a *cis*-restricted phenomenon: gene silencing is more pronounced at the locus that was originally exposed to dsRNA. We propose that an RNAi-directed chromatin mark is deposited at the *gfp* locus and that this mark sensitizes genes to long-term silencing. H3K9me3 is an excellent candidate for such a mark.

Heritable RNAs are also required for RNAi inheritance: the siRNA-binding protein HRDE-1 is required each and every generation to maintain heritable RNAi silencing (Fig. 1d). Thus, RNA and chromatin marks both seem to promote RNAi inheritance. Why might this be? In *S. pombe*, the RNAi machinery induces H3K9me3 at genomic loci targeted by siRNAs. Concurrently, the H3K9me3 chromatin mark helps localize the RNAi machinery to these same genomic loci: Thus, a self-reinforcing loop of chromatin modifying and RNAi silencing machinery coordinately induces RNAi silencing in *S. pombe* (7,8). We propose that a similar process likely occurs in *C. elegans*: RNAi directs H3K9me3, and H3K9me3 helps recruit RNAi machinery to H3K9me3 containing loci. Thus, the role of H3K9me3 in heritable gene silencing may be to sensitize loci to silencing by heritably expressed siRNAs. Further work is needed to test this idea.

RdRPs and RNAi inheritance. RNAi silencing in *C. elegans* can last for more than five generations. Adult *C. elegans* produce ~250 progeny. Therefore, F5 inheriting progeny would be expected to inherit a vanishingly small fraction of an initial RNAi silencing signal. Thus, the ability of *C. elegans* to "remember" RNAi silencing events that occurred in previous generations is likely an active process. Consistent with this idea, we find that heritable siRNA levels do not decrease by 250x each generation after dsRNA exposure even though the population size grows by 250x each generation (see Fig. 1c, and Fig. S8). HRDE-1 associates with 22G siRNAs (Fig. S11), and 22G siRNAs are synthesized by RNA dependent RNA Polymerases (RdRPs) (9-11). Thus, it seems reasonable to speculate that HRDE-1 siRNAs are made by RdRPs and that RdRPs could act to maintain pools of heritable siRNAs (by synthesizing new 22G siRNAs) each generation. This model predicts that germline transcription would be a pre-requisite for long-term RNAi inheritance: germline transcription would be required to provide mRNA templates for

RdRPs each generation. Consistent with this idea, dsRNAs that target genes that are not expressed in germ cells (but are expressed in somatic cells) fail to induce RNAi inheritance that persists for more than one generation (12,13).

Endogenous versus exogenous heritable RNAi silencing. Here we show that exogenously provided dsRNA mediates heritable silencing that is lost in the first generation that animals lack HRDE-1 or NRDE-2 (Fig. 1d, Table S1, and Fig. 2b). These data suggest that heritable silencing triggered by exogenous dsRNAs is lost immediately in animals lacking the downstream (receiving) components of the RNAi inheritance machinery. Loss of heritable silencing at endogenous germline target genes, however, occurs gradually after loss of the RNAi inheritance machinery (Fig. 3f, Fig. S14-15). We do not understand why RNAi silencing at endogenous target genes is more intransigent to the loss of the RNAi inheritance machinery than exogenous silencing. Perhaps this distinction arises from differences in the history of silencing at these loci. Germline target genes are subjected to heritable silencing for many generations. In our exogenous RNAi experiments genes are subjected to silencing for only one or two generations. It is possible that long-term silencing alters chromatin states in a way that makes gene silencing relatively recalcitrant to loss of the RNAi inheritance machinery. Alternatively, germline target genes might produce "aberrant" RNAs, which harbor intrinsic silencing promoting characteristics that make gene silencing at these loci relatively resistant to loss of the RNAi inheritance machinery. Finally, redundant Agos, or redundant silencing pathways, could conceivably contribute to heritable silencing at endogenous, but not exogenous, targets genes.

RNAi inheritance and germline immortality. The RNAi inheritance machinery transmits endogenous epigenetic information across generational boundaries while promoting germline immortality (Fig. 3 and 4, Fig. S14-16). We do not understand how defects in epigenomic maintenance relate to defects in germline immortality. We consider three models that might explain the link between epigenomic maintenance and germline immortality. Model #1: *S. pombe* that lack the RNAi machinery exhibit chromosome segregation defects that are thought to be due to a failure of these mutant cells to impart the appropriate chromatin states to centromeres (14). We have found that late generation RNAi inheritance defective (henceforth termed "mortified") animals exhibit Him phenotypes that becomes progressively more severe after disabling the RNAi inheritance machinery (Fig. S19). High incidence of males (Him) phenotypes in *C. elegans* typically arise due to nondisjunction of X chromosomes during meiosis (15). Thus, Mrt could be due to meiotic chromosome segregation defects in mortified animals. Model #2: among HRDE-1 associated siRNAs are siRNAs that target a subset of *C. elegans* transposons. For instance, Tc4 and Tc5 siRNAs associate with HRDE-1 (Table S2). Thus, Mrt might be caused by transposon mobilization in mortified germ cells. Model #3: Loss of the RNAi inheritance machinery alters gene expression programs in germ cells that, over generations, become progressively more severe. Thus, Mrt could be caused by over-expression of germline target genes that eventually reaches levels that are incompatible with germ cell function. Further work is needed to test these models.

Supplemental data:

Table S1. HRDE-1 acts in inheriting progeny to promote multi-generational RNAi inheritance. *pos-1* RNAi induces an embryonic arrest phenotype, which is heritable (4). P0 hermaphrodites of the indicated genotypes were treated with *pos-1* dsRNA at a dose that permitted between 10-30% of F1 offspring to survive. Hermaphrodites of the indicated genotypes were selfed (**A**) or crossed to males of the indicated genotypes (**B**). F1 offspring were reared in the absence of dsRNA and % arrest of F2 embryos was scored. *hrde-1* chromosome in P0 hermaphrodites was marked with *dpy-17* (*dpy-17* is ~1.5 cM from *hrde-1*), and F1 cross progeny (**B**) and *hrde-1* genotype in F2 animals (**A-B**) and were inferred by presence/absence of Dpy phenotypes. NA, not applicable. Number in brackets indicates # of embryos scored.

P0 hermaphrodite genotype (*pos-1* RNAi)	P0 male genotype (no *pos-1* RNAi)	F1 genotype	F2 % embryonic arrest
A			
+/+	NA (selfed)	+/+	64% (1564)
hrde-1(-)/hrde-1(-)	NA (selfed)	*hrde-1(-)/hrde-1(-)*	5% (1536)
hrde-1(-)/ +	NA (selfed)	*hrde-1(-)/hrde-1(-)*	3% (1614)
		hrde-1(-)/+ or +/+	57% (1162)
B			
hrde-1(-)/hrde-1(-)	*hrde-1(-)/hrde-1(-)*	*hrde-1(-)/hrde-1(-)*	2% (883)
hrde-1(-)/hrde-1(-)	+/+	*hrde-1(-)/+*	47% (2730)

Table S2 (see attached excel spreadsheet). List of putative HRDE-1 target loci. Genes (column geneName) are ranked by # of HRDE-1 siRNAs (column HRDE1coIPsiRNA). Sequences of HRDE-1 co-IP small RNAs were aligned to mRNA sequences of all *C. elegans* genes (SW190). An rpkm (reads per kilobase per million total reads) value was calculated for each gene by counting the number of HRDE-1 co-IP small RNAs that perfectly match to the antisense strand of mRNA sequence, followed by normalizations by the size of mRNA (kb) and the total number of sequenced reads. Columns of H3K9me3_N2, H3K9me3_nrde2, and H3K9me3_nrde4 indicate fold H3K9me3 enrichment (ratios of H3Kme3 IP to input) for each gene in N2, *nrde-2(gg091),* and *nrde-4(gg129)* populations, respectively. The column (*nrde-2/4* dependent H3K9me3) indicates whether or not H3K9me3 level of a HRDE-1 target gene is dependent on wild type expression of *nrde-2 and nrde-4.* To be considered a *nrde-2/4*-dependent gene, H3K9me3 levels in both *nrde-2* and *nrde-4* mutant populations had to be equal or less than half of H3K9me3 level in the N2 population. This analysis was conducted for the top 500 HRDE-1 target genes. Note: many genes homologous to HRDE-1 bound siRNAs did not exhibit loss of H3K9me3 in *nrde-2/4(-)* animals. These data could indicate that targeting by HRDE-1 endo siRNAs is not always sufficient to induce H3K9me3, or, may reflect differences in developmental stage of animals used to prepare HRDE-1 siRNA (mixed stage), and *nrde-2/4(-)* H3K9me3 (adult), sequencing libraries (see also Fig S12). In the main text we state that there are ~1500 HRDE-1 target genes. We arbitrarily defined HRDE-1 target genes as those genes having > 50 HRDE-1 siRNAs (rpkm). Genes with less than 50 siRNAs are colored in red in this table. **(Sheet 1)** The first sheet of this spreadsheet (see above) shows HRDE-1 siRNAs that match predicted genes. Sheet 1 shows intergenic regions (cryptic loci) of the genome that are complementary to HRDE-1 bound siRNAs. (**Sheet 2**) Sheet 2 shows pseudogenes that are complementary to HRDE-1 bound siRNAs.

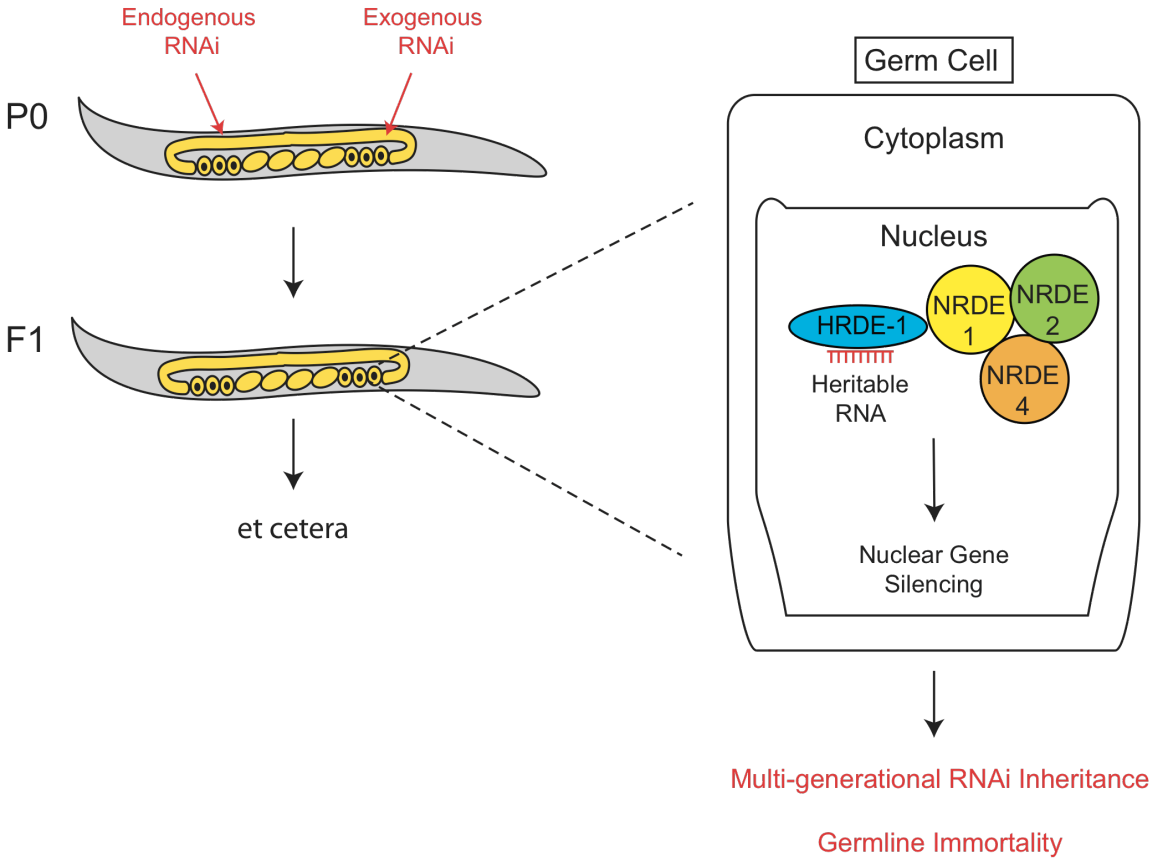

Fig. S1. Model. HRDE-1 acts in germ cell nuclei of inheriting generations to drive nuclear RNAi, propagate multi-generational RNAi silencing signals, and promote germline immortality. Nrde interaction surfaces are hypothetical.

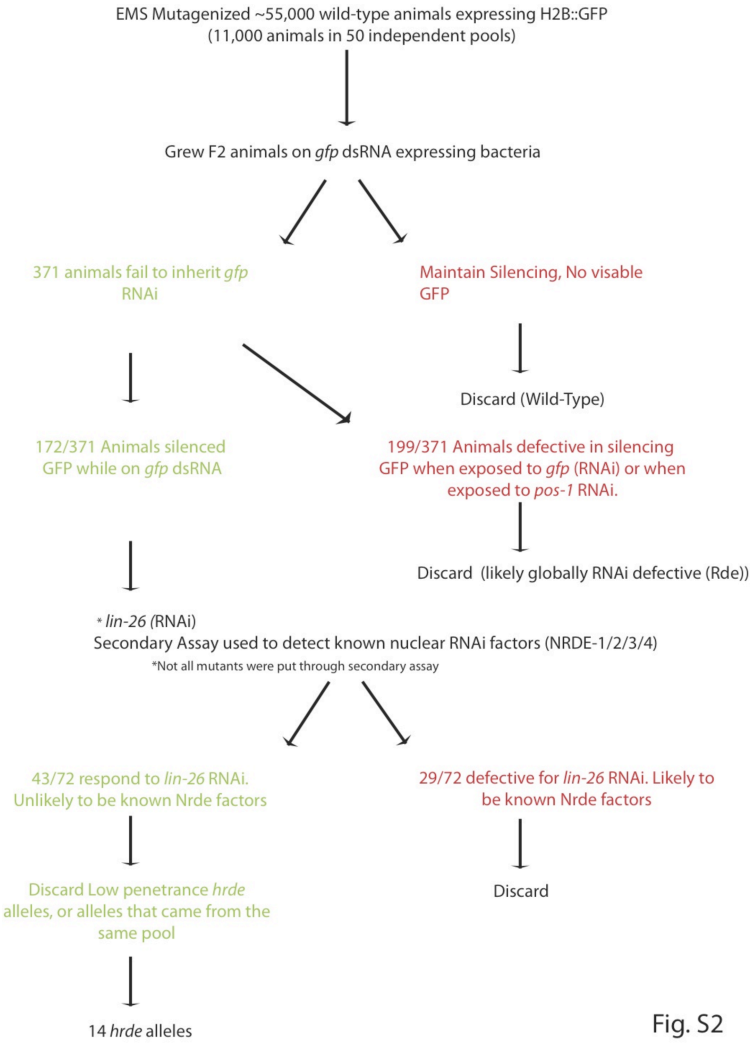

Fig. S2

Fig. S2. Genetic screen for *hrde* alleles. *pie-1::gfp::h2b* animals were mutagenized with EMS. F2 progeny of these mutagenized animals were subjected to *gfp* RNAi. F3 progeny were scored for GFP expression. Mutant animals unable to inherit *gfp* RNAi silencing were kept for further analysis. As a secondary screen, we tested these mutants for their ability to silence *gfp* when exposed directly to *gfp* dsRNA. We discarded mutants that failed to silence *gfp* when exposed directly to *gfp* dsRNA. We also tested mutants for suppression of *pos-1* RNAi-mediated lethality when exposed directly to *pos-1* dsRNA. We discarded mutants that suppressed *pos-1* RNAi. These two secondary screens were used to identify mutant animals unable to respond to dsRNA when directly exposed to dsRNA (likely representing animals with global defects in RNAi silencing). Next we used *lin-26* RNAi in an attempt to identify and eliminate mutants harboring alleles of *nrde-1/2/3/4*. *lin-26* RNAi induces a lethal phenotype in wild-type animals. *nrde-1/2/3/4(-)* animals fail to respond to *lin-26* RNAi when directly exposed to *lin-26* dsRNA. Mutant animals that were defective for *lin-26* RNAi were discarded. Note: it is possible that these secondary screens may have prevented our identification of some genes involved in multi-generational RNAi inheritance. Of the remaining 43 mutant strains, we chose a single mutant from each pool, which exhibited highly (>90%) penetrant RNAi inheritance defects (14 total) for further analysis.

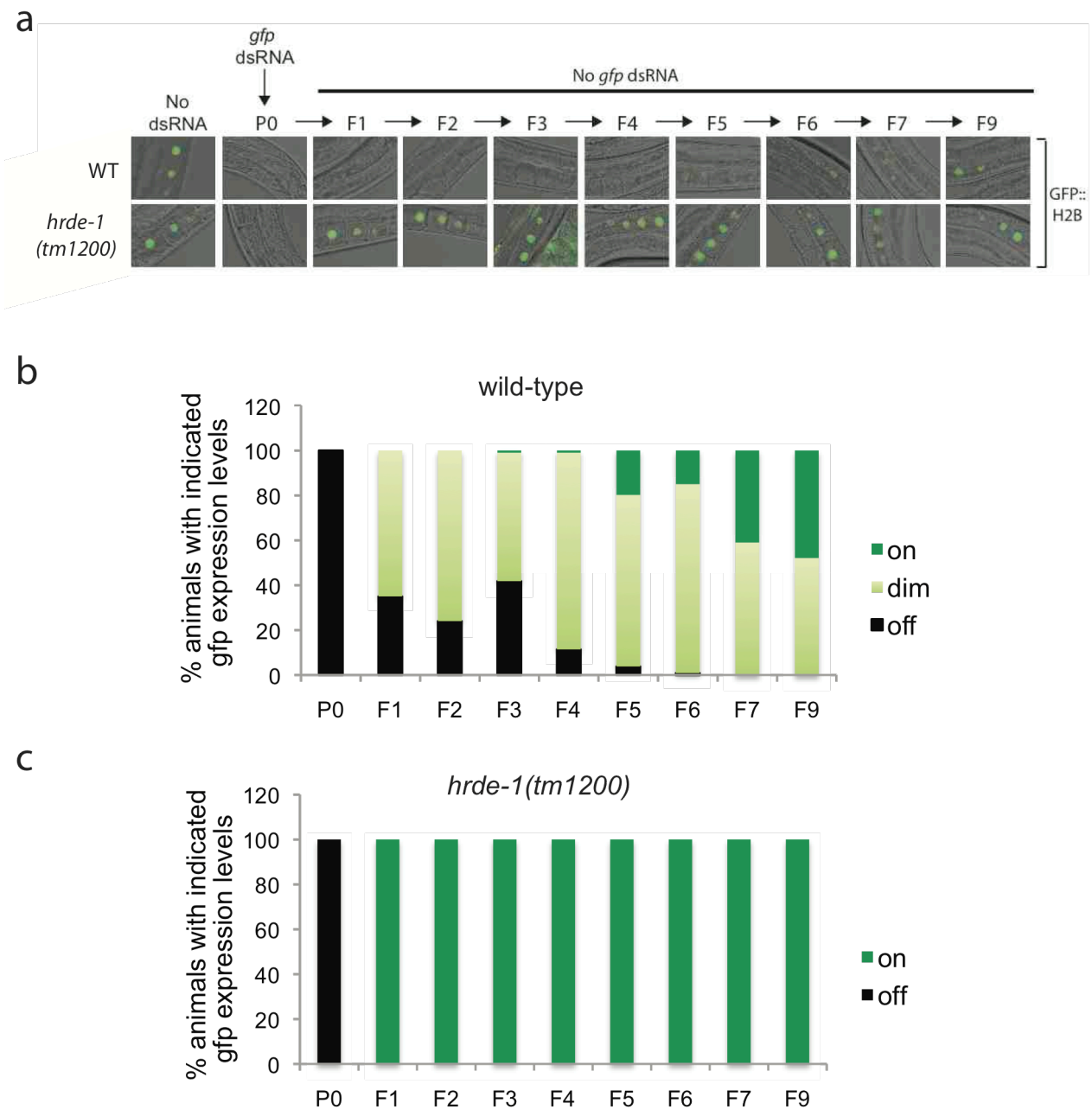

Fig. S3. Multi-generational perdurance of *gfp* silencing in *pie-1::gfp::h2b* expressing animals (+ or – HRDE-1). (a) *pie-1::gfp::h2b* expressing animals (+/- *hrde-1*) were exposed to *gfp* dsRNA in the P0 generation. Fluorescent images of GFP expression in the P0 and inheriting generations are shown. **(b)** *pie-1::gfp::h2b* expressing animals, which were exposed to *gfp* dsRNA in the P0 generation, were scored visually as (off) no *gfp* expression, (dim) some *gfp* expression- but lower than animals never exposed to *gfp* dsRNA, and (on) similar to animals never exposed to *gfp* dsRNA. Note: many animals scored as "dim" were very dim. When images were taken of these animals (at the same exposure time as "On" animals) no fluorescence could be seen in images. For instance, Fig. 1a and Fig. 2a show F1 progeny of wild-type animals exposed to *gfp* dsRNA. Some of these animals might have been scored as dim, but no GFP fluorescence is visible in image. This experiments was repeated 3 times and similar results were seen in each experiment.

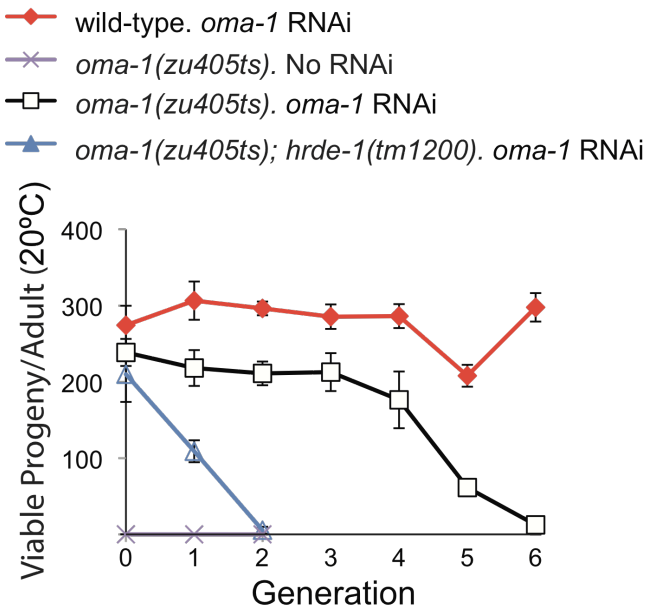

Fig. S4. HRDE-1 is required for heritable silencing of *oma-1*. *zu405ts* is a temperature sensitive (ts) lethal (embryonic arrest at 20ºC) allele of *oma-1* (16). *oma-1* RNAi suppresses *oma-1(zu405ts)* lethality, and this effect is heritable (5). P0 animals were exposed to *oma-1* RNAi and number of viable progeny in the indicated generations was scored (20ºC). n=3-6, +/- s.e.m). *oma-1* dsRNA is sufficient to silence *oma-1(zu405ts)* for five generations: viable animals were observed for five generations after *oma-1* dsRNA treatment. HRDE-1(-) animals are defective for inheritance of *oma-1* silencing. Note: some RNAi inheritance was seen in the F1 progeny of *hrde-1(-)* animals exposed to *oma-1* dsRNA, suggesting that in certain cases some RNAi inheritance can occur in the absence of HRDE-1.

a

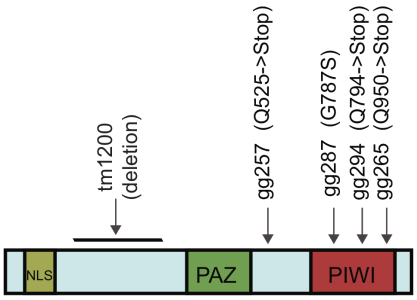

b

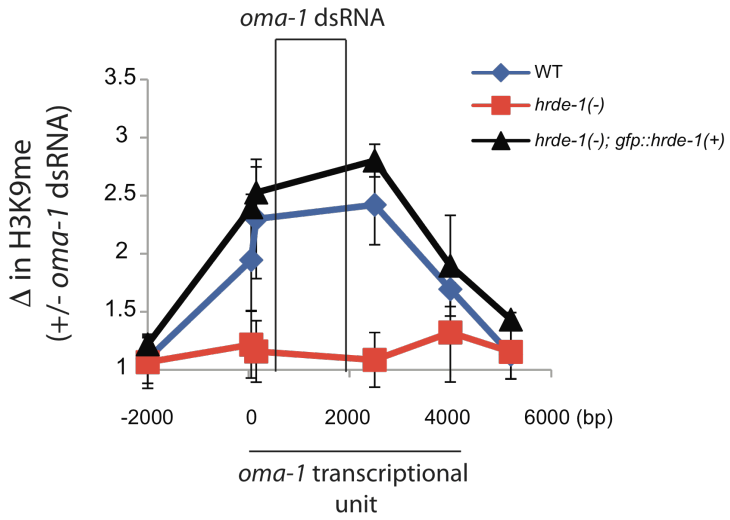

Fig. S5. ***hrde-1 is c16c10.3***. **(a)** We mapped *hrde-1* to a region of chromosome three that contained the gene *c16c10.3*. Sequencing identified mutations within *c16c10.3* coding regions in each of the four *hrde-1* alleles identified in our genetic screen. Complementation analyses further support that *hrde-1 is c16c10.3*: *hrde-1* alleles identified in our genetic screen failed to complement a deletion allele of *c16c10.3* for RNAi inheritance defects (data not shown). Predicted domain structure of HRDE-1 protein is shown. *hrde-1* alleles are indicated by arrows. **(b)** In Fig. 2d and Fig. S10, we show that *oma-1* dsRNA induces H3K9me3 at the *oma-1* gene, which is heritable and *hrde-1*-dependent. In panel **(b)** we show that a wild-type copy of *c16c10.31* expressed in *hrde-1(-)* animals rescues this *hrde-1* associated RNAi inheritance defect, confirming the molecular identify of *hrde-1*. *c16c10.31* fused to *gfp* (*gfp::hrde-1)* was integrated into the genome and this transgene was then crossed into *hrde-1(tm1200)* animals and *hrde-1(tm1200); gfp::hrde-1* animals were isolated. Animals of the indicated genotypes were exposed to *oma-1* dsRNA and F1 progeny were subjected to H3K9me3 ChIP at 20ºC. Co-precipitating DNA was quantified with qRT-PCR. Data were normalized to co-precipitating *eft-3* DNA and expressed as a ratio +/- *oma-1* RNAi (1=no change). X-axis, 0 denotes predicted start codon of *oma-1*. (D), fold change. (bp), base pair. (n=3, +/- s.e.m.).

a

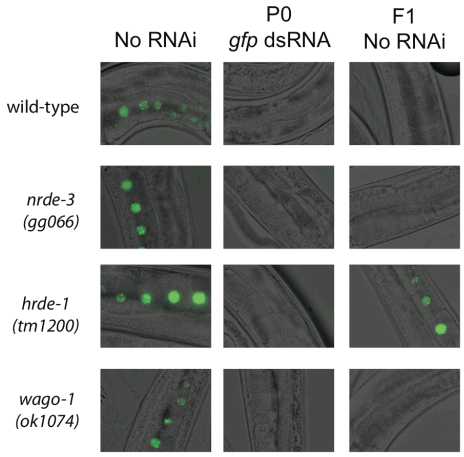

b

HRDE-1 may be the only WAGO required for
pie-1::gfp::h2b RNAi inheritance

		RNAi inheritance defective lines			
WAGO		**Line 1**	**Line 2**	**Line 3**	**Line 4**
1	r06c7.1	wt	wt	wt	wt
2	f55a12.1	wt	wt	wt	wt
3	ppw-2	wt	wt	wt	wt
4	f58g1.1	wt	wt	wt	wt
5	zk1248.7	wt	wt	het	wt
6	sago-2	wt	het	het	wt
7	ppw-1	wt	del?	del?	?
8	sago-1	wt	wt	wt	wt
9	hrde-1	del	del	del	del
10	t22h9.3	wt	wt	wt	wt
11	y49f6a.1	het	wt	het	wt
12	nrde-3	wt	del	?	wt

Fig. S6. *hrde-1* may be the only WAGO able to promote multi-generational *gfp* RNAi inheritance. (a) Animals harboring predicted null alleles in three wagos (*hrde-1, nrde-3,* and *wago-1*) and expressing *pie-1::gfp::h2b* were subjected to *gfp* RNAi inheritance assays. Of these three wagos, only *hrde-1* was defective for germline RNAi inheritance **(b)** The *wago-12* strain harbors deletion alleles in all twelve *C. elegans wago* genes (10). We crossed the integrated *pie-1::gfp::h2b* transgene into the *wago-12* strain. Four independent F2 RNAi inheritance defective lines were isolated. This strategy was repeated two more times. PCR was then used to genotype the twelve *wagos*. *hrde-1* segregated with the RNAi inheritance defect in all four lines. The *pie-1::gfp::h2b* transgene is linked (~2 centimorgans) to *hrde-1* (data not shown). Thus, in the first cross we had a ~20x better chance of picking another wago contributing to RNAi inheritance than *hrde-1* because identifying *hrde-1* required a recombination event between *hrde-1* and *pie-1::gfp::h2b* (no other *wago* is linked to *pie-1::gfp::h2b*). In the next two crosses, the odds of picking *hrde-1* over any another *wago* contributing strongly to RNAi inheritance were ½. So the chance of our having isolated *hrde-1* in all four independent times (if another *wago* contributes strongly to RNAi inheritance) are $(1/20)^4$ x $(1/2)^4$ x $(1/2)^4$= ~1/40,000,000. Note: this argument assumes that the twelve *wago* deletion alleles used in this study represent strong loss of function alleles. In addition, some *oma-1* RNAi inheritance was observed in the F1 progeny of *hrde-1(-)* animals exposed to *oma-1* dsRNA (Fig. S4), suggesting that other *wagos* might contribute to RNAi inheritance when genes other than the *pie-1::gfp::h2b* transgene are targeted by dsRNA.

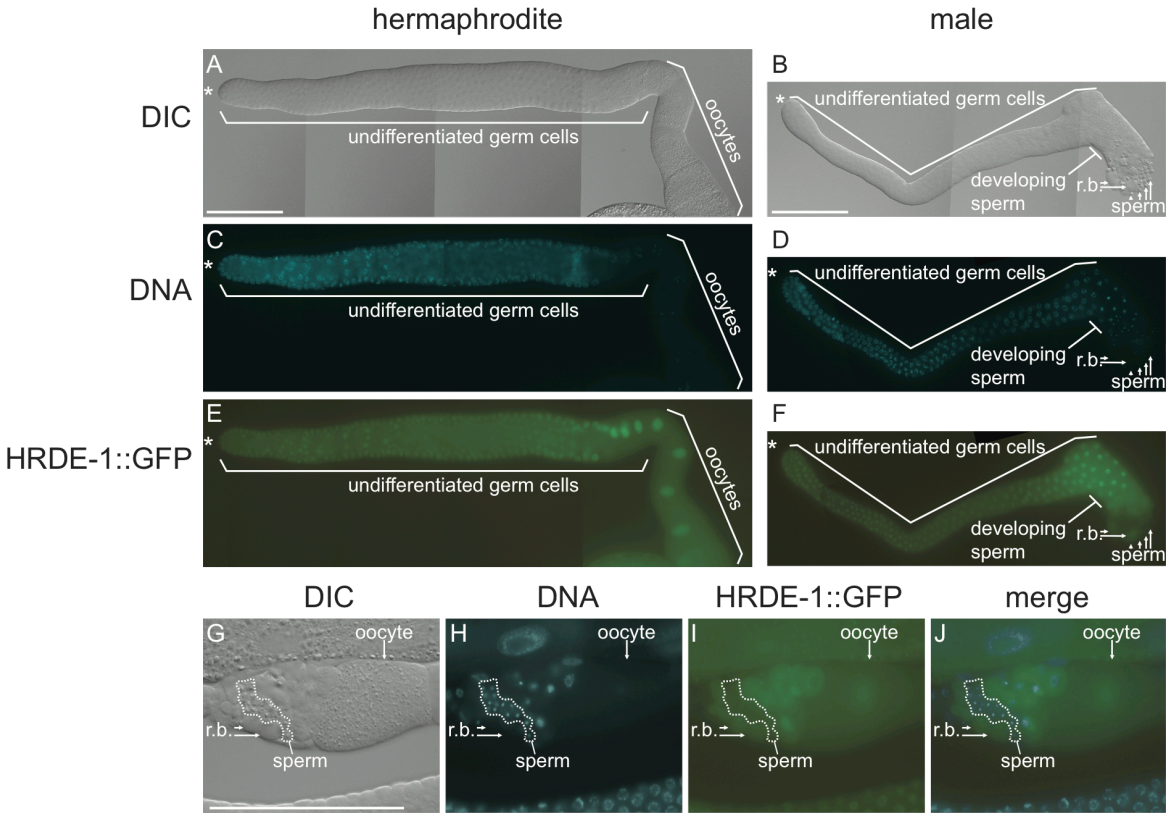

Fig. S7. HRDE-1::GFP is expressed in nuclei of female germ cells, and in nuclei of developing sperm. (a-j) Gonads from hermaphrodites and males expressing HRDE-1::GFP were dissected, fixed, DAPI stained, and imaged for GFP and for DNA. **(a,c,e)** In hermaphrodite gonads, HRDE-1::GFP is expressed broadly in undifferentiated germ cells and in oocytes. HRDE-1::GFP expression is virtually identical to the DNA stain, indicating HRDE-1::GFP localizes to nuclei. Gonad was dissected from an adult hermaphrodite grown to 24 h post-L4 stage. Asterisk marks the germline distal end. **(b,d,f)** In males gonads, HRDE-1::GFP is also broadly expressed in undifferentiated germ cells and in spermatocytes (developing sperm), and HRDE-1::GFP expression is virtually identical to the DNA stain, indicating HRDE-1::GFP nuclear localization. However, HRDE-1 is present at low levels, or is absent from, differentiated sperm. HRDE-1::GFP is, however, present in residual bodies (r.b.), cytoplasmic material left over after spermatogenesis. Gonad was dissected from an L4 male. Asterisk marks the germline distal end. **(g-j)** In young adult hermaphrodite gonads, HRDE-1 is present in residual bodies, but is present at low levels in or is absent from differentiated sperm. Shown is a magnified image of an adult hermaphrodite proximal gonad shortly after the L4-to-adult molt. All scale bars are equal to 100μm.

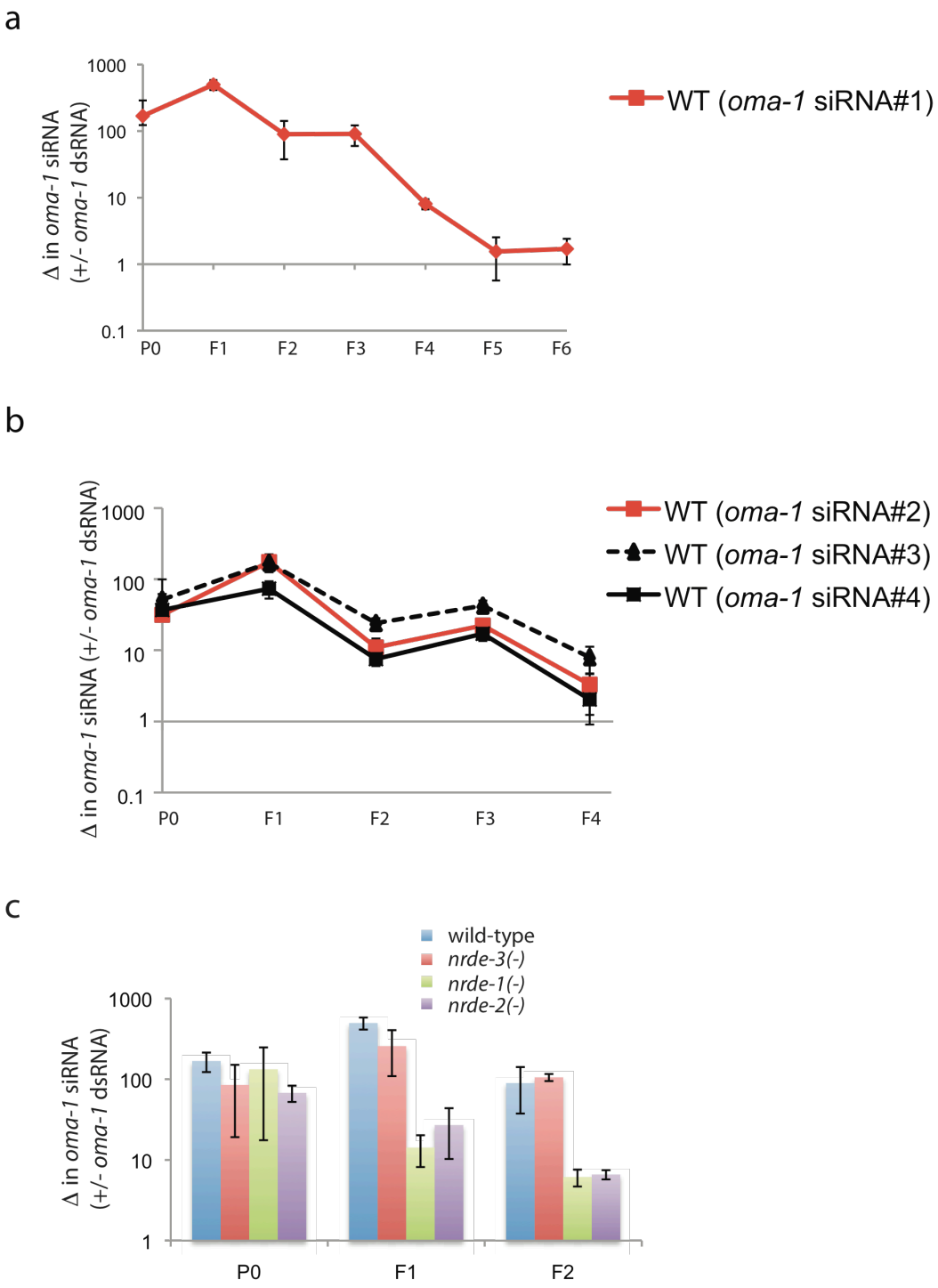

Fig. S8. *oma-1* siRNAs are inherited for multiple generations. (a) RNA was isolated from animals (and the progeny of these animals) treated with *oma-1* dsRNA. *oma-1* siRNA was quantified using a TaqMan probe set. Data were normalized to *eft-3* RNA and expressed as ratio (+/- *oma-1* RNAi). (D), fold change. (n=3-4, +/- s.e.m.). **(b)** Three additional custom-made TaqMan probe sets were used to quantify *oma-1* siRNAs. Two of these probe sets detect secondary siRNAs. Data were normalized to *eft-3* RNA and expressed as ratio (+/- *oma-1* RNAi). (n=3-4, +/- s.e.m.). The sequences targeted by *oma-1* TaqMan probes were *oma-1* #1 GAACAAGTCTTAGATTCGAGCC, *oma-1* #2:GATGTGCTGCTCCATTTGATCA, *oma-1* #3: GAGACAAGTCCTTAGCGTGATC, *oma-1* #4: GATCTTCTCGTTGTTTTCACCG. **(c)** *oma-1* siRNAs are initially produced in RNAi inheritance mutant animals but are not maintained in inheriting progeny. TaqMan *oma-1* probe set was used to quantify *oma-1* siRNA as described in Fig. 1c (n=3-4, +/- s.e.m.).

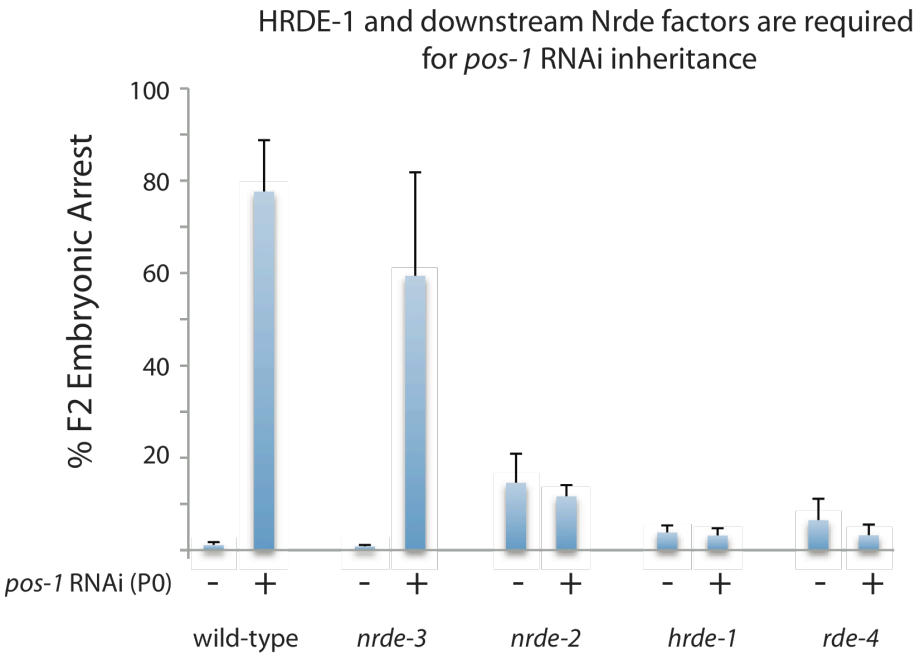

Fig. S9. HRDE-1 and a downstream Nrde factor are required for *pos-1* RNAi inheritance (a) Animals of the indicated genotypes were exposed to *pos-1* dsRNA at a concentration that produced >50% F1 lethality. Surviving F1 progeny were grown in the absence of *pos-1* dsRNA and % F2 embryonic arrest was scored.

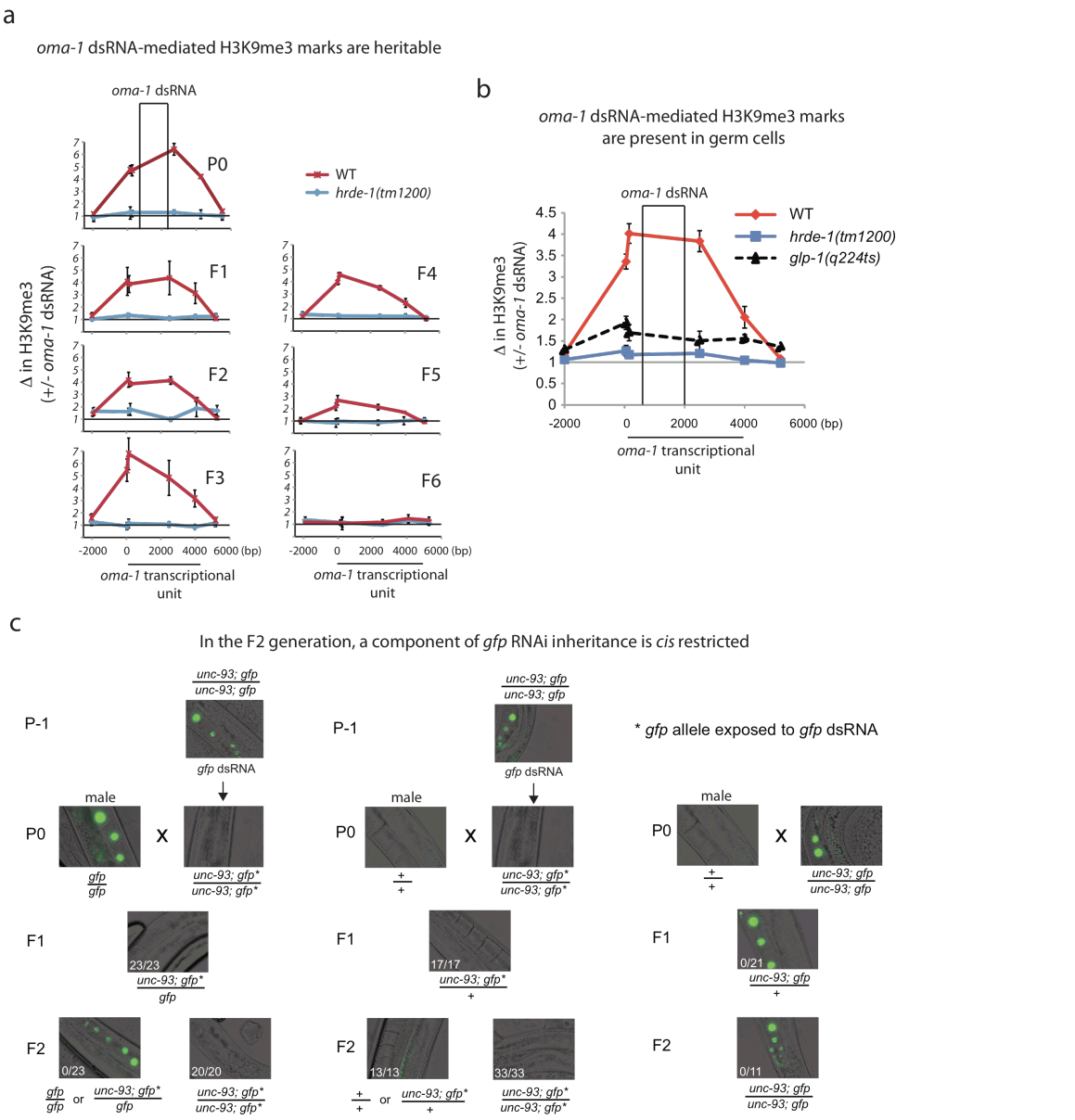

Fig. S10. dsRNA-mediated H3K9me3 is HRDE-1 dependent, heritable, and likely sensitizes genomic loci to siRNA-mediated gene silencing. (a) Animals were exposed to *oma-1* dsRNA for two generations (2nd generation is defined as P0) and F1 progeny were subjected to H3K9me3 ChIP at 20ºC. Note: similar results were seen after one generation of *oma-1* dsRNA treatment. Co-precipitating DNA was quantified with qRT-PCR. Data were normalized to co-precipitating *eft-3* DNA and expressed as a ratio +/- *oma-1* RNAi (1=no change). X-axis, 0 denotes predicted start codon of *oma-1*. (D), fold change. (bp), base pair. (n=3-4, +/- s.e.m.). **(b)** Animals harboring the temperature sensitive *glp-1(q224ts)* allele produce a substantially reduced set of germ cells at 25ºC (17). Animals of indicated genotypes (+/- *hrde-1* or +/- *glp-1(q224ts)* were exposed to *oma-1* dsRNA. H3K9me3 co-precipitating DNA was quantified in F1 progeny with qRT-PCR. Data were normalized to co-precipitating *eft-3* DNA and expressed as a ratio +/- *oma-1* RNAi (1=no change). X-axis, 0 denotes predicted transcriptional start site of *oma-1*. (D), fold change. (bp), base pair. (n=3-4, +/- s.e.m.). **(c)** Animals expressing *pie-1::gfp::h2b* marked with *unc-93* were exposed to *gfp* or control dsRNA for two generations and then mated with males of the indicated genotypes that had not been exposed to *gfp* dsRNA. Heterozygous F1 cross progeny (inferred by +/- Unc phenotype) were visualized for oocyte *gfp* expression by fluorescence microscopy. F1 cross progeny were allowed to self and *gfp* expression in F2 self-progeny was scored. Genotypes were inferred by presence/absence of Unc phenotype. * indicates *gfp* allele was exposed to *gfp* dsRNA in the P0 generation. The number of animals that exhibited no (or faint) GFP expression is indicated. Note: while not obvious from the images shown in **(c)**, we could detect both *cis* and *trans* silencing effects in F2 inheriting generations in these experiments. In independent reproductions of this experiment, *cis* and *trans* silencing were reproducibly observed but the relative contribution *cis* and *trans* effects to overall silencing differed.

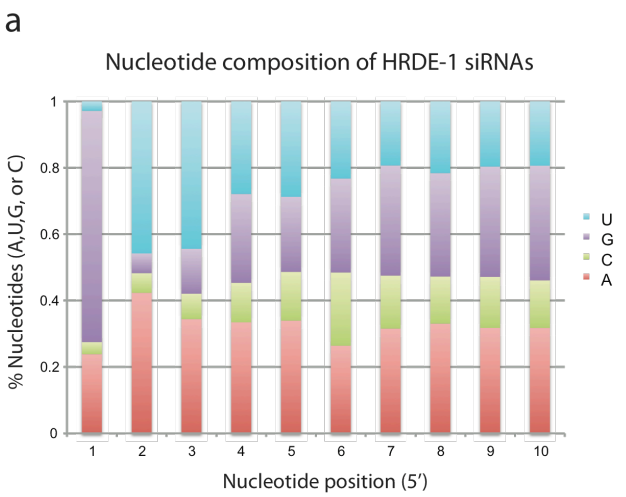

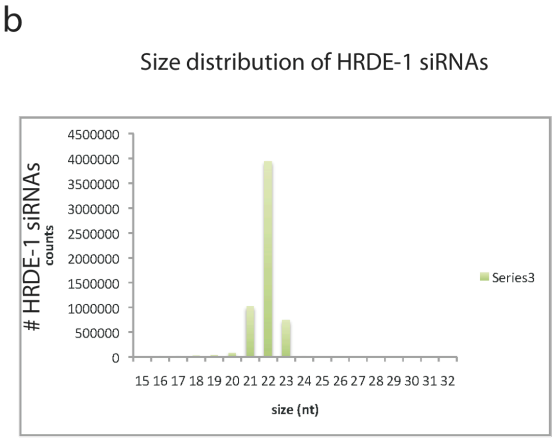

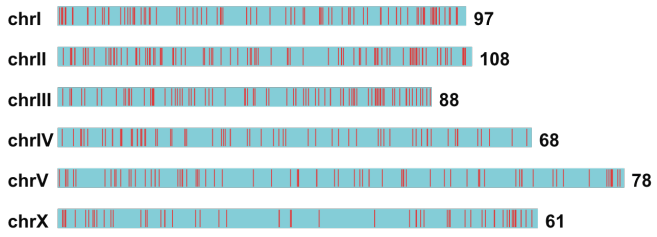

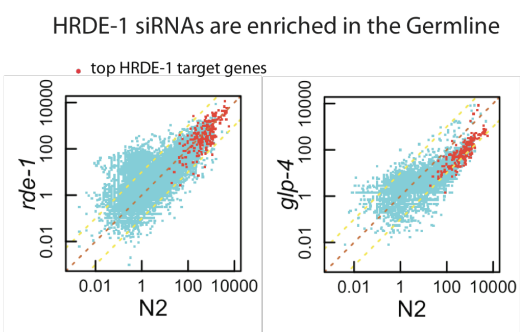

e

HRDE-1 22G siRNAs target genes that also produce oocyte/embryo 26G siRNAs

Gene Name	# HRDE-1 22G siRNAs	Top 1000 HRDE-1 target gene?	
C40A11.10	547	yes	Oocyte/Embryo 26G target genes
E01G4.7	337	yes	
F39E9.7	167	yes	
F55C9.5	53	no	
fbxb-37	125	yes	
K02E2.6	337	yes	
T05E12.8	308	yes	
T25G12.11	104	yes	
W05H12.2	933	yes	
Y37E11B.2	824	yes	
Y82E9BR.20	33	no	
C04G2.8	2	no	Sperm 26G target genes
C32E8.4	13	no	
deps-1	10	no	
dlc-6	6	no	
gska-3	21	no	
msp-49	0	no	
sod-1	9	no	
ssp-16	0	no	
ssp-19	0	no	
T08B2.12	1	no	
ZC168.6	1	no	
ZK484.5	3	no	

Fig. S11. HRDE-1 associates with 22G endo siRNAs that are expressed in germ cells. (a) The nucleotide composition (1= 5' most nucleotide) of HRDE-1 siRNAs is shown. **(b)** Nucleotide length (nt) of HRDE-1 co-precipitating RNAs is shown. **(c)** Chromosomal locations of the top 500 HRDE-1 target loci are indicated with red lines (chr, chromosome). **(d)** siRNAs were sequenced from wild-type (N2) and *glp-4(bn2)* at 25°C (few germ cells present in *glp-4(bn2)* animals at this temperature). Gene-based scatter plot representation of siRNA reads at 20,937 *C. elegans* genes. Top 200 HRDE-1 target genes are shown in red. **(e)** 22G siRNAs target many loci that also produce 26G siRNAs (18). We asked if HRDE-1 22G siRNAs targeted loci that also produce 26G siRNAs. We found that genes targeted by 26G siRNAs in oocytes/embryos were also targeted by HRDE-1 22G siRNAs. Genes targeted by 26G siRNAs in sperm did not appear to be targeted by HRDE-1 22G siRNAs (18). Finally, we analyzed eight control genes, which do not produce 26G siRNAs in either oocytes or sperm and found that none of these loci were among the top 1000 HRDE-1 target genes (data not shown).

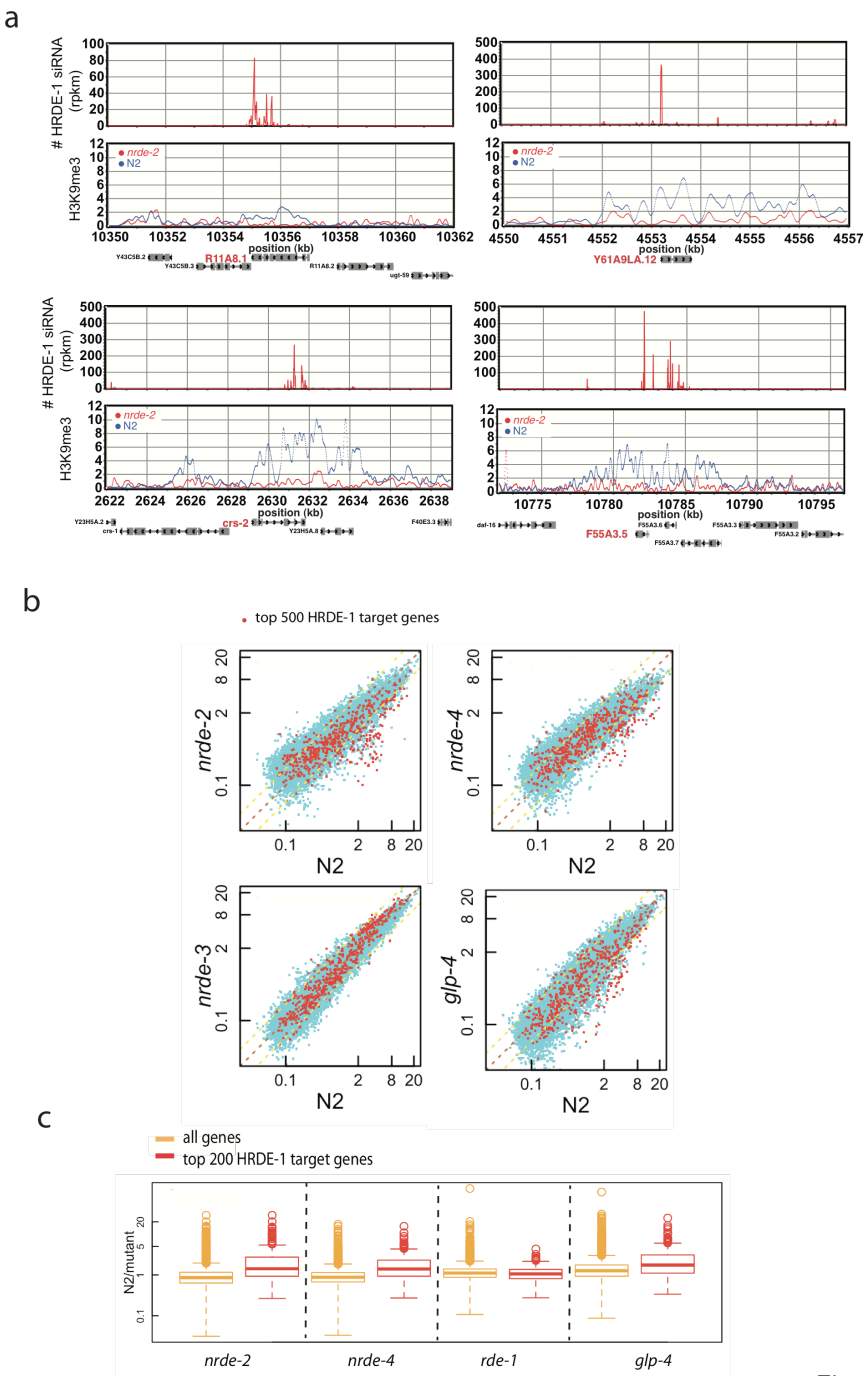

Fig. S12. Overlap between HRDE-1 siRNA targeted loci and *nrde-2/4*-dependent H3K9me3 loci. (a) HRDE-1 siRNAs and NRDE-2-dependent H3K9me3 at four germline target genes. Small RNA levels (Top panels) and H3K9me3 levels (Bottom panels) were plotted according to position on chromosome. **(b)** A gene-based scatter plot representation of H3K9me3 in mutant (y-axis) vs. wild-type (N2) (x-axis). All genes (blue) and top 500 HRDE-1 target genes (red). Animals were treated with *smg-1* dsRNA as a positive control (19). N2 and *nrde-2* H3K9me3 chip-seq data were published previously (NCBI GEO database (accession number: GSE32631) (19). **(c)** Box plot representation of the relative change of H3K9me3 at all *C. elegans* genes or the top 200 genes targeted by HRDE-1 siRNAs. Data is shown as a ratio of H3K9me3 in wild-type (N2) /mutant animals. Note: (**b,c**) show that many HRDE-1 target genes do not exhibit loss of H3K9me3 in *nrde-2/4(-)* animals. These data could indicate that targeting by HRDE-1 endo siRNAs is not always sufficient to induce H3K9me3, or, may reflect differences in developmental stage of animals used to prepare HRDE-1 siRNA (mixed stage), and *nrde-2/4(-)* H3K9me3 (adult), sequencing libraries.

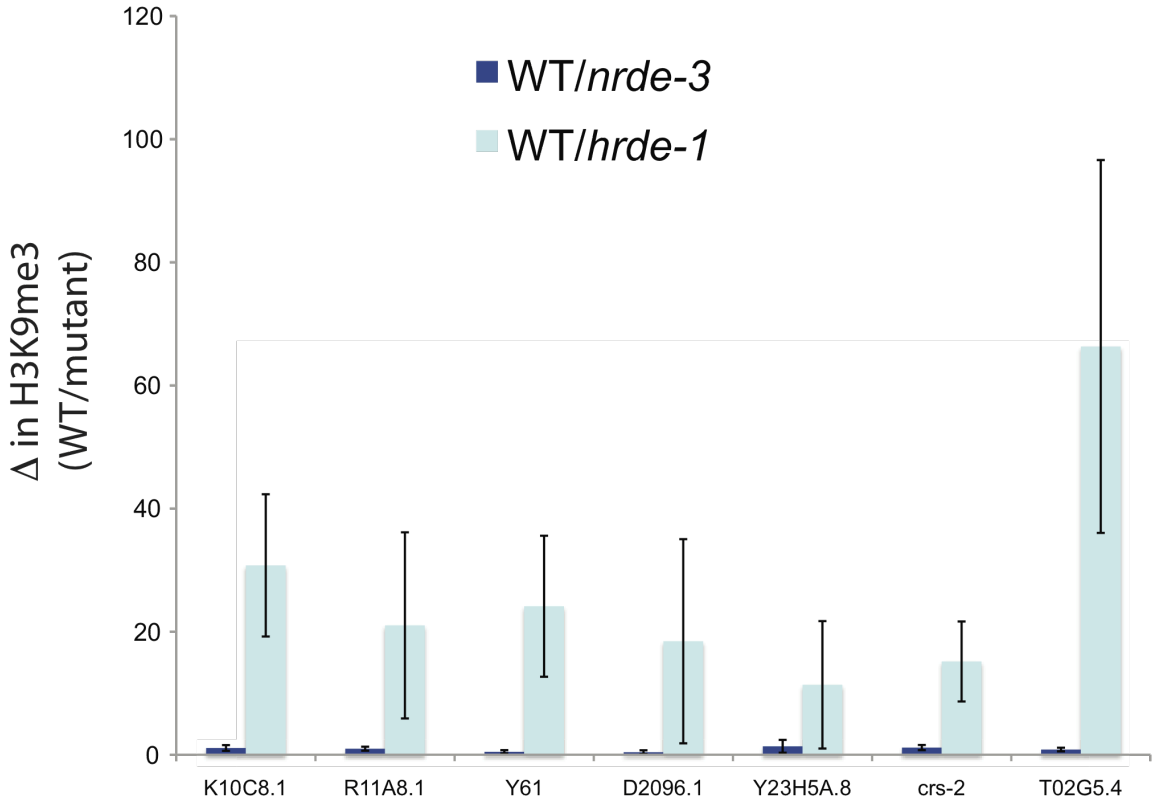

Fig. S13. Germline target genes are depleted for H3K9me3 in *hrde-1(-)*, but not *nrde-3(-)*, animals. qRT-PCR quantification of H3K9me3 ChIP at seven germline target genes from animals ((wild-type, *hrde-1(tm1200)*, and *nrde-3(gg066)*) grown at 20°C. Data were normalized to co-precipitating *eft-3* DNA and expressed as a ratio WT/mutant (n=2-6, +/- s.e.m.). Note: values >1 indicate less H3K9m3 in mutant animals versus wild-type.

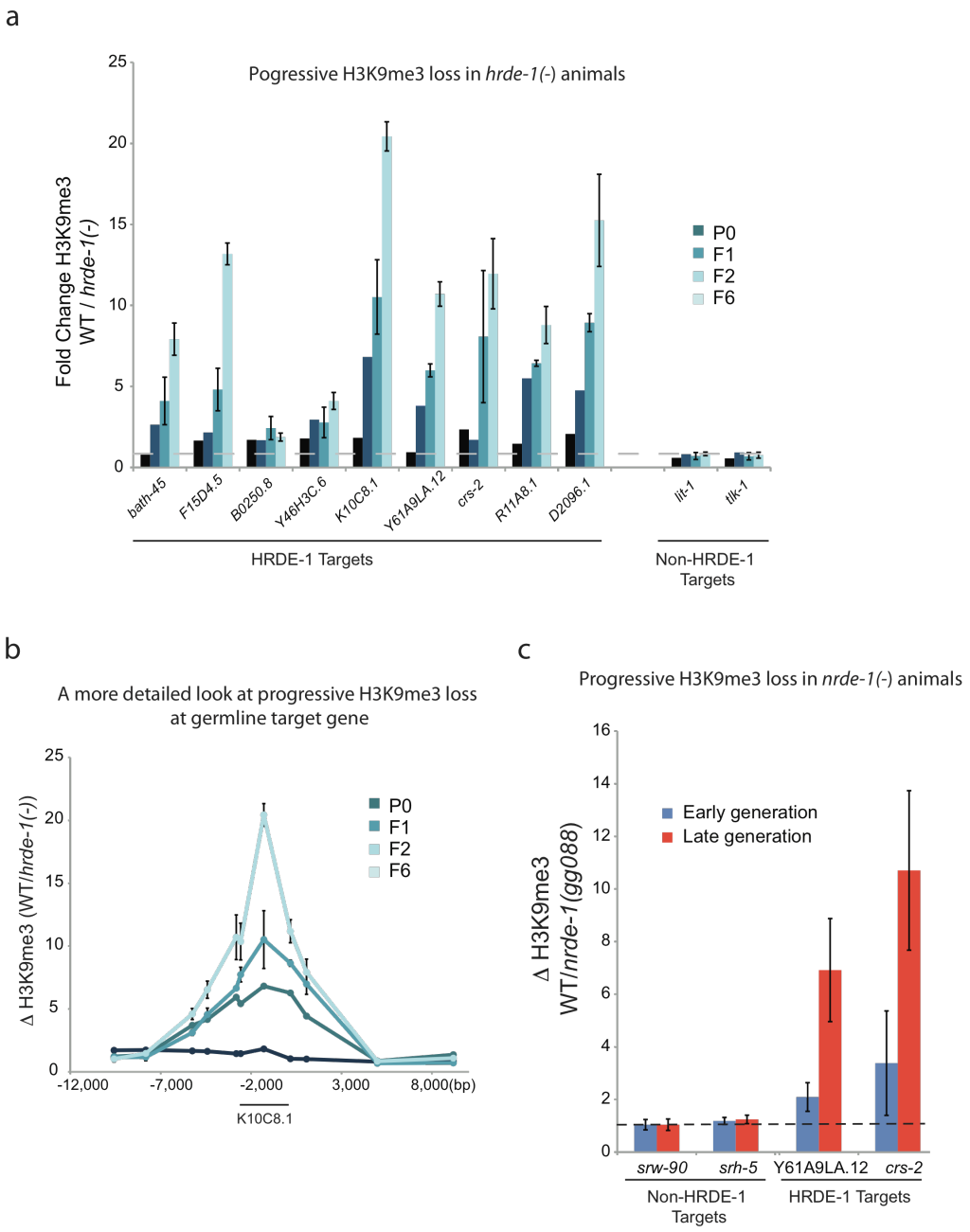

Fig. S14. Late generation *hrde-1(-)* or *nrde-1(-)* animals exhibit more pronounced H3K9me3 loss than early generation animals. (a) *dpy-17* is linked (~1.5 cM) to *hrde-1*. *dpy-17* or *hrde-1; dpy-17* animals were out-crossed 5x, and Dpy adult animals (P0) and adult progeny (F1, F2, F6) were isolated and H3K9me3 at HRDE-1 target genes was quantified with qRT-PCR **(a)** detecting nine genes targeted by HRDE-1 siRNAs (HRDE-1 target genes) or **(b)** multiple primer pairs surrounding a single HRDE-1 targeted gene (K10C8.1). **(a)** Two genes, which are not targeted by HRDE-1 siRNAs, but exhibit Nrde-independent H3K9me3 in the germline, were used as negative controls (non-HRDE-1 targets). Data are expressed as a ratio (WT/*hrde-1*) (n=1 for P0-F1, and n=3 for F2 and F6, +/- s.e.m.). **(c)** *nrde-1(-)* animals were out-crossed to wild-type 4x and early generation *nrde-1(-)* homozygous animals (F3) and late generation (>F10) animals were subjected to H3K9me3 ChIP. H3K9me3 was quantified at two control genes (no HRDE-1 siRNAs) and two germline target genes (HRDE-1 siRNAs). (n=2-4, +/- s.e.m.). Co-precipitating DNA was quantified with qRT-PCR. Data were normalized to co-precipitating *eft-3* DNA and expressed as a ratio WT/*nrde-1(-)*. (**a,b,c**) Animals were grown at 20°C.

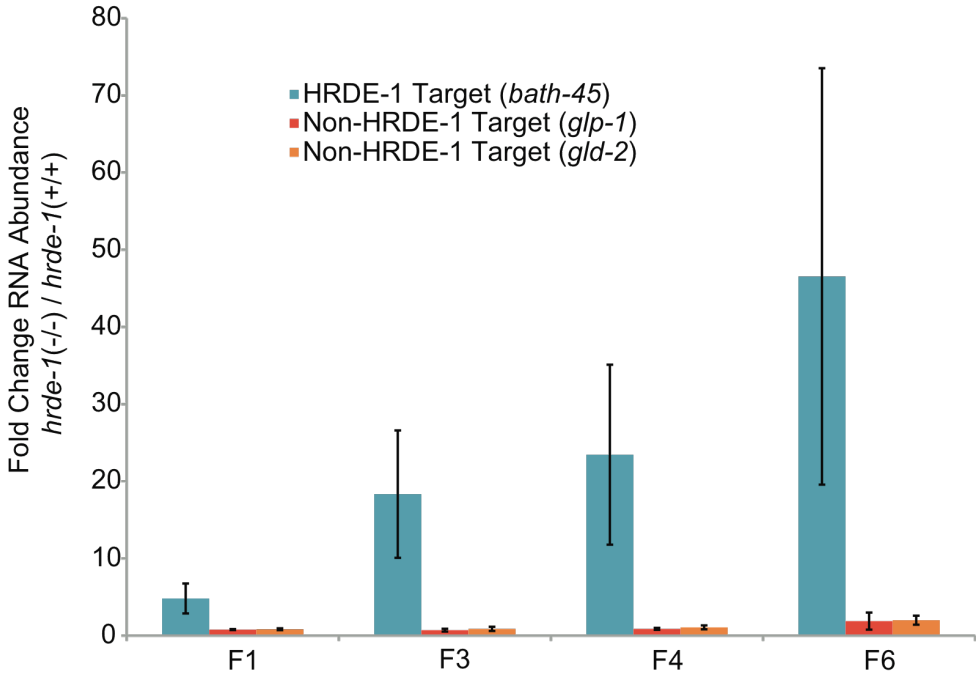

Fig. S15. Germline target gene mis-regulation becomes more pronounced in late generation *hrde-1(-)* animals. RNA isolated from *hrde-1(-/-)* and *hrde-1(+/+)* siblings of the indicated generation was converted to cDNA and quantified with qRT-PCR detecting one HRDE-1 target gene and two non HRDE-1 target genes (n=4 for F1, n=5 for F4, n=3 for F4, and n=2 for F6; +/- sem).

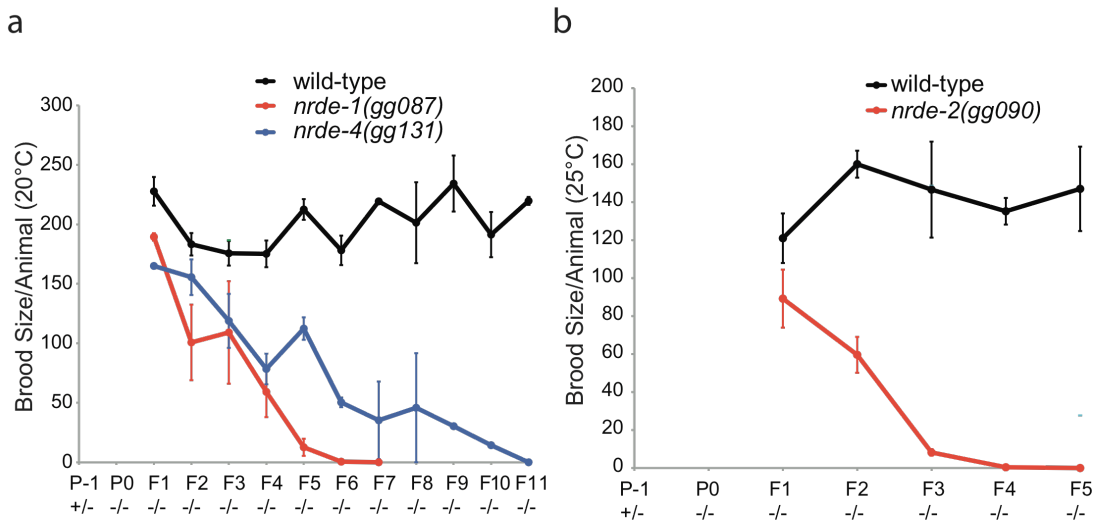

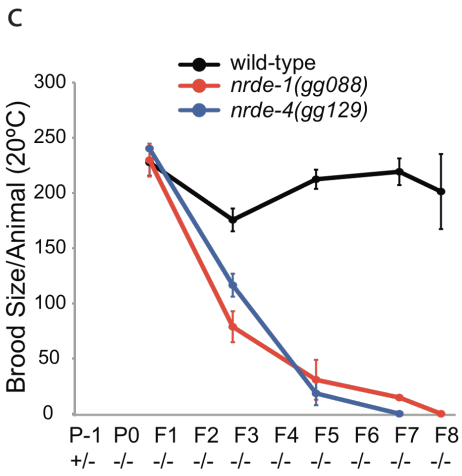

d

	Generation				
	1	2	3	4	5
control	+	+	+	+	+
hrde-1(gg257)	+	+	+	+	-
hrde-1(gg265)	+	+	+	+	-
hrde-1(gg287)	+	+	+	+	-

Fig. S16. Mutations in *hrde-1* or *nrde-1/2/4* induce a mortal germline (Mrt) phenotype. (**a-c**) Animals of indicated genotypes were out-crossed to wild-type 4x and brood sizes scored across generations. (**d**) Three *hrde-1* alleles identified in our genetic screen were grown at 25°C, and the generation at which these strains (*hrde*; *pie-1::gfp::h2b*) became sterile is noted. (-) indicates no progeny were observed on plates. (+) indicates progeny were observed. Control is *pie-1::gfp::h2b.* For **a** n=3-7, for **b** n=5, for **c** n=3-5, +/- s.e.m.). The wild-type data in **(b)** are the same as in Figure 4 of the main text.

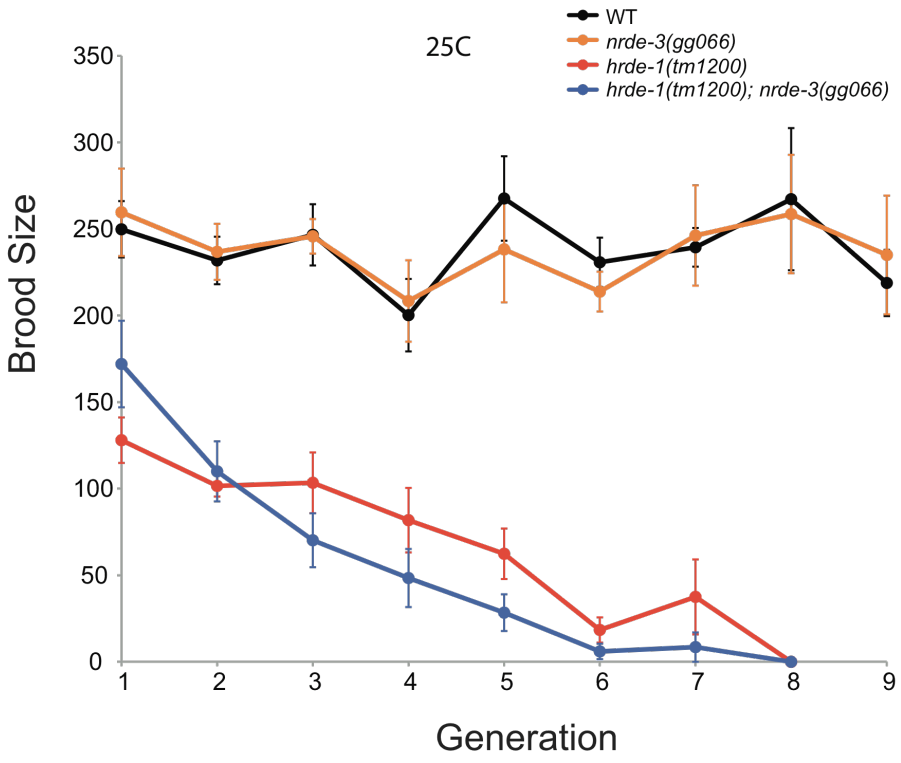

Fig. S17. Animals lacking the somatic Ago NRDE-3 do not exhibit a germline Mrt phenotype. Wild-type and *nrde-3(gg066)* (predicted null allele of *nrde-3*) animals were grown at 25°C and brood sizes were scored at the indicated generations. (n=5, +/- s.e.m.). In addition, a strain harboring predicted null alleles in both *nrde-3* and *hrde-1* behaved similarly to *hrde-1* mutant animals for Mrt, indicating that *nrde-3* does not contribute appreciably to germline immortality.

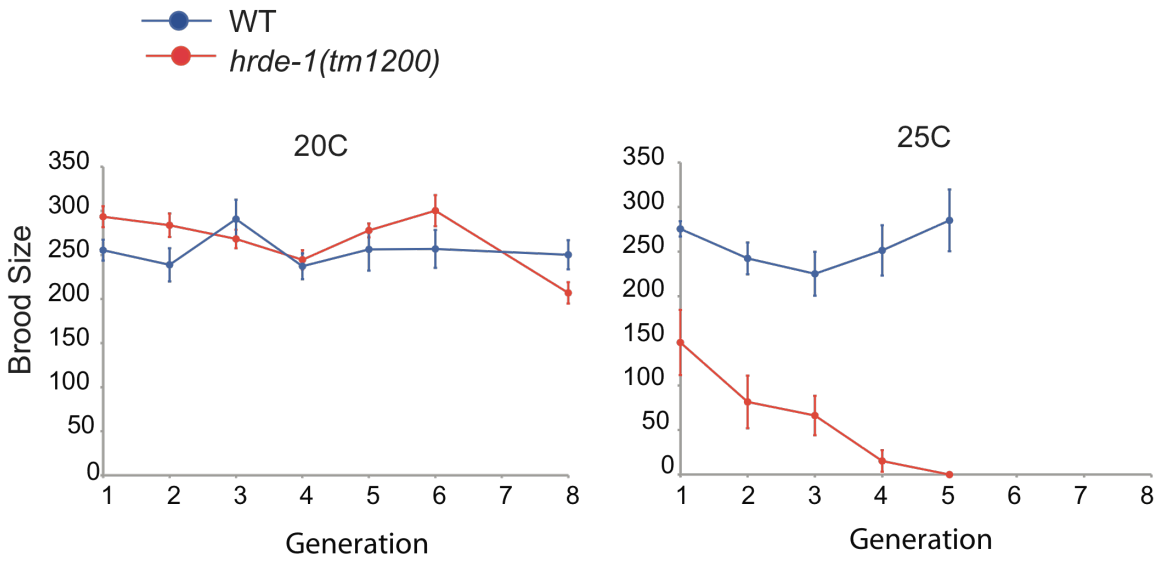

Fig. S18. The Mrt phenotype of *hrde-1(-)* animals is temperature sensitive. Animals of the indicated genotypes were grown at the indicated temperatures and brood sizes were scored across generations (n=10, +/- s.e.m.).

a

	germ cells present	generation F1(n)	F3(n)	F4(n)	F5(n)
+/+	sperm + oocytes	100% (33)	95% (20)	89% (25)	100% (40)
	sperm only	0%	0%	7% (2)	0%
	oocytes only	0%	5% (1)	4% (1)	0%
	no differentiated gametes	0%	0%	0%	0%
hrde-1/hrde-1	sperm + oocytes	100% (24)	87% (14)	47% (15)	26% (6)
	sperm only	0%	13% (2)	41% (13)	35% (8)
	oocytes only	0%	0%	0%	9% (2)
	no differentiated gametes	0%	0%	12% (4)	30% (7)

b

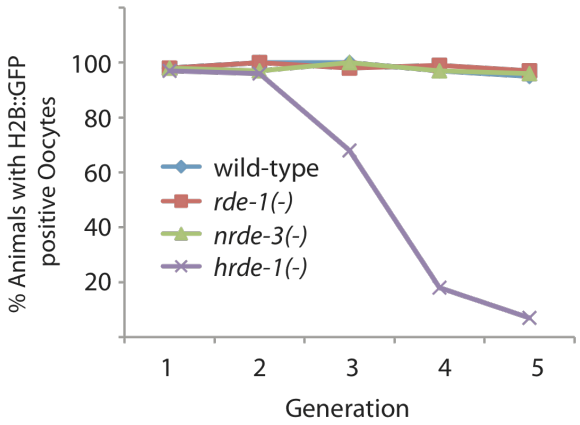

c

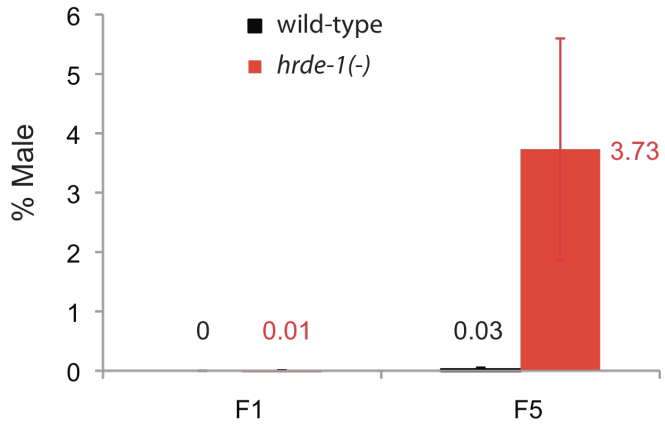

Fig. S19. Late generation *hrde-1(-)* animals fail to produce mature gametes and exhibit a Him phenotype. (a) *hrde-1(+/+)* and *hrde-1(-/-)* siblings were isolated from a *hrde-1(+/-)* parent and F1-F5 progeny (grown at 25°C) were scored for oocyte and sperm as described in Fig. 4b. **(b)** *pie-1::gfp::h2b* is expressed in nuclei of oocytes. *pie-1::gfp::h2b* expressing animals were grown at 25°C and the % of animals of the indicated genotypes that possessed wild-type looking oocytes at the indicated generations were scored. **(c)** *hrde-1(-/-)* or *hrde-1(+/+)* siblings were grown 25°C and the percentage of male progeny in the indicated generation was scored (n+3, +/- s.e.m). HRDE-1(-) animals exhibited a High incidence of males (Him) phenotypes, suggesting that late generation RNAi inheritance defective animals might exhibit defects in meiotic chromosome segregation (see supplemental discussion).

Supplemental Materials and Methods:

Strain list:
(YY513) pkIS32[pie-1p::gfp::h2b], (YY528) hrde-1(tm1200);pkls32, N2 (CGC), (YY563) hrde-1(gg265);pkIS32, (YY516) rde-1(ne219);pkIS32, (TX20) oma-1(zu405), (YY562) hrde-1(tm1200); oma-1(zu405), (YY557) ggIS053 [hrde-1p::3xflag::gfp::hrde-1], (YY542) unc-93(e1500);pkIS32, (YY543) hrde-1(tm1200); unc-93(e1500),pklS32, (YY538) hrde-1(tm1200), (YY514) nrde-1(gg088);pklS32, (YY492) nrde-2(gg091);pkIS32, (YY515) nrde-4(gg129); pkIS32, (YY573) wago-1(ok1074); pkIS32(YY158) nrde-3(gg066), (YY160) nrde-1(gg088), (YY186) nrde-2(gg091), (WM49) rde-4(ne301), (YY554) hrde-1(tm1200); nrde-2(gg091);ggIS28[nrde-3p::3xflag::gfp::nrde-2], (YY346) nrde-2(gg091);ggIS28, (JK1107) glp-1(q224ts), (YY453) nrde-4(gg129), (JK4630) qis174, (YY560) hrde-1(tm1200);ggIS053, WM191 sago-2(tm894); ppw-1(tm914); ppw-2(tm1120); F44A12.1(tm2686); R06C7.1(tm1414); Y49F6.1(tm1127), ZK1248.7(tm1113); F58G1.1(tm1019)II; C16C10.3(tm1200); K12B6.1(tm1195); T22H9.3(tm1186)V; RO4A9.2(tm1116), (YY187) nrde-1(gg087), (YY410) nrde-4(gg131), (YY185) nrde-2(gg090), (YY564) hrde-1(gg257);pkl32, (YY565) hrde-1(gg287), (MH1870) kuIS54 (sur-5p:::gfp), (YY518) nrde-1(gg088);kuIS54, (YY520) nrde-3(gg066); kuIS54, (YY521) nrde-4(gg129); kuIS54, (YY548) hrde-1(tm1200); kuIS54, (YY529) hrde-1(tm1200); nrde-3(gg066) pkIS32, (YY545) hrde-1(tm1200); nrde-3(gg066), (RB1096) wago-1(ok1074), (CB164) dpy-17(e164), (YY544) hrde-1(tm1200); dpy-17(e164), (SS104) glp-4(bn2).

HRDE-1 endo siRNA sequencing. HRDE-1 co-IP small RNAs were captured using a 5'-monophosphate-independent method and sequenced on an Illumina GAIIX platform (11). For Table S2, sequences of HRDE-1 co-IP small RNAs were aligned to mRNA sequences of all *C. elegans* genes (SW190). An rpkm (reads per kilobase per million total reads) value was calculated for each gene by counting the number of HRDE-1 co-IP small RNAs that perfectly match to the reverse complementary strand of mRNA sequence, followed by normalizations by the size of mRNA (kb) and the total number of sequenced reads (million). For Figure 3c and Fig. S12a, sequences of HRDE-1 co-IP small RNAs were aligned to the *C. elegans* genome (SW190). siRNA coverage (rpkm) at any given position was calculated by dividing the number of siRNAs (ones that match to the antisense strand of the target gene) that cover this position by the number of total alignments (in millions). If a read matches to multiple places in the genome, a fraction (1/the number of matches) was used to calculate the siRNA coverage.

H3K9me3 Seq. Wild-type and NRDE-2 H3K9me3 chip-seq data used in this study were from a previous study (19) (NCBI GEO database (accession number: GSE32631). After removing barcodes, 25-nt reads were aligned to the *C. elegans* genome (SW190) using Bowtie. Only perfect alignments were used for analysis. For Figure 3c and Fig. S12a, nucleosome cores were modeled as 147 bases of sequences, extending from the first base of alignment. Nucleosome coverage at any given position was calculated by dividing the number of nucleosome cores that cover this position by the number of total alignments (in millions). If a read matches to multiple places in the genome, a fraction (1/the number of matches) was used to calculate the nucleosome coverage.

Construction of *gfp::hrde-1*. For FLAG::GFP::HRDE-1 the predicted *hrde-1* promoter was amplified from N2 genomic DNA with primers (5'-taattacgtcgaCCCGTATCCTTGAC 5'-taattacgtcgaCAAACGATGCGAAT), digested

with SalI, and inserted into pSG081 5' of 3xFLAG::GFP (pBB001). The *hrde-1* coding region and predicted 3'UTR were then amplified by PCR from genomic N2 DNA with primers (5'-taattagggcccAAGTCAAACATGGC and 5'-taattagggcccCGTGCAATGTAATA), digested with ApaI, and inserted into pBB001 3' to the hrde-1p::3xFLAG::GFP. Low copy integrated transgenes were generated by biolistic transformation (20).

***oma-1* RNAi Assay**. 6-10 L1 animals of indicated genotypes were picked to oma-1 RNA at 20C (restrictive temperature), this was designated the P0 generation. They were allowed to lay broods and total brood size was counted when F1 animals became gravid. 6-10 F1 animals were picked, as L1s, to OP50. This process was repeated for subsequent generations. (Note: As brood size decreased over generations there was in increase in unhatched eggs laid, this was not quantified.)

***oma-1* siRNA TaqMan assay**. TaqMan assay was performed as described previously (12). TaqMan assays were designed to quantify the following small RNA sequences: oma-1 #1: GAACAAGTCTTAGATTCGAGCC, oma-1 #2:GATGTGCTGCTCCATTT GATCA, oma-1 #3: GAGACAAGTCCTTAGCGTGATC, oma-1 #4: GATCTTCTC GTTGTTTTCACCG. Note probes set #1 and #2 detect siRNAs derived from sequences targeted by *oma-1* dsRNA in P0 animals. Probe sets #3 and #4 detect secondary siRNAs (sequences not directly targeted by *oma-1* dsRNA).

HRDE-1 endo siRNA detection. To isolate HRDE-1 associated siRNAs mixed stage animals were sonicated in lysis buffer (20 mM Tris-HCl, pH 7.5, 200 mM NaCl, 2.5 mM $MgCl_2$, and 0.5% NP-40). Lysates were clarified by centrifuging at 14k rpm for 15 min. Supernatants were pre-cleared with Protein G agarose beads (Roche) and incubated with anti-FLAG M2 agarose (Sigma) beads for 1 hour at 4ºC. Beads were washed extensively and FLAG::GFP::HRDE-1 was eluted with 100 ug/ml 3xFLAG peptide (Sigma). Eluates were incubated with 5 volumes of TRIzol reagent (Invitrogen), followed by isoproponal precipitation. Precipitates were treated with calf intestinal alkaline phosphatase (CIAP, Invitrogen) at 37^{o}C for 30 min, re-extracted with TRIzol, and treated with T4 polynucleotide kinase (T4 PNK, New England Biolabs) together with γ-[32]p-ATP at 37ºC for 30 min.

cDNA preparation. For Fig. 2c and Fig. 3e, RNAs isolated by TRIzol extraction were converted to cDNA by the iScript cDNA Synthesis Kit (Bio-Rad, 170-8890) following the vendor's protocol.

Mrt assay. Unless otherwise indicated, mutant alleles were out-crossed with wild-type (N2) 4 times and mutant allele was re-isolated as a homozygote. At each generation, 6 larval stage (L1) animals were picked to a single plate. Average brood sizes were calculated by counting the total number of progeny per plate.

Immunocytochemistry. Antibody staining of dissected gonads was carried out essentially as described elsewhere (Jones, Francis, Schedl, 1996). Briefly, dissected gonads were fixed in 3% paraformaldehyde, 100mM K_2HPO_4 (pH 7.2) for 1 hours at room temperature, and then permeabilized in 100% methanol at -20°C. Samples were washed three times in PBST (PBS + 0.1% Tween-20) and blocked in PBST + 0.5% BSA for 30 min at room temperature. The sperm-specific mouse antibody SP56 (1:100 dilution in PBST + 0.5% BSA) (21) and the oocyte-labeling rabbit anti-RME-2 antibodies (1:500 dilution) (22) primary antibodies were incubated at 4°C overnight. Cy3 and Cy5 conjugated secondary

antibodies (1:500 dilution, Jackson ImmunoResearch) were incubated for 1-2 hours at room temperature along with 4',6-diamidino-2-phenylindole (DAPI) (0.5 ug/ml) to visualize DNA. For visualizing GFP, gonads from HRDE-1::GFP expressing animals were fixed and permeablized as mentioned above, and then stained with DAPI. All imaging was carried out using Zeiss Axio Imager D1 microscope.

Supplemental Bibliography:

(1) Moazed D. Small RNAs in transcriptional gene silencing and genome defence. Nature 2009 Jan 22;457(7228):413-420.
(2) Guang S, Bochner AF, Burkhart KB, Burton N, Pavelec DM, Kennedy S. Small regulatory RNAs inhibit RNA polymerase II during the elongation phase of transcription. Nature 2010 Jun 24;465(7301):1097-1101.
(3) Burkhart KB, Guang S, Buckley BA, Wong L, Bochner AF, Kennedy S. A pre-mRNA-associating factor links endogenous siRNAs to chromatin regulation. PLoS Genet 2011 Aug;7(8):e1002249.
(4) Grishok A, Tabara H, Mello CC. Genetic requirements for inheritance of RNAi in C. elegans. Science 2000 Mar 31;287(5462):2494-2497.
(5) Alcazar RM, Lin R, Fire AZ. Transmission dynamics of heritable silencing induced by double-stranded RNA in Caenorhabditis elegans. Genetics 2008 Nov;180(3):1275-1288.
(6) Vastenhouw NL, Brunschwig K, Okihara KL, Muller F, Tijsterman M, Plasterk RH. Gene expression: long-term gene silencing by RNAi. Nature 2006 Aug 24;442(7105):882.
(7) Noma K, Sugiyama T, Cam H, Verdel A, Zofall M, Jia S, et al. RITS acts in cis to promote RNA interference-mediated transcriptional and post-transcriptional silencing. Nat Genet 2004 Nov;36(11):1174-1180.
(8) Sugiyama T, Cam H, Verdel A, Moazed D, Grewal SI. RNA-dependent RNA polymerase is an essential component of a self-enforcing loop coupling heterochromatin assembly to siRNA production. Proc Natl Acad Sci U S A 2005 Jan 4;102(1):152-157.
(9) Pak J, Fire A. Distinct populations of primary and secondary effectors during RNAi in C. elegans. Science 2007 Jan 12;315(5809):241-244.
(10) Gu W, Shirayama M, Conte D,Jr, Vasale J, Batista PJ, Claycomb JM, et al. Distinct argonaute-mediated 22G-RNA pathways direct genome surveillance in the C. elegans germline. Mol Cell 2009 Oct 23;36(2):231-244.
(11) Gent JI, Schvarzstein M, Villeneuve AM, Gu SG, Jantsch V, Fire AZ, et al. A Caenorhabditis elegans RNA-directed RNA polymerase in sperm development and endogenous RNA interference. Genetics 2009 Dec;183(4):1297-1314.
(12) Burton NO, Burkhart KB, Kennedy S. Nuclear RNAi maintains heritable gene silencing in *Caenorhabditis elegans*. PNAS 2011.
(13) Fire A, Xu S, Montgomery MK, Kostas SA, Driver SE, Mello CC. Potent and specific genetic interference by double-stranded RNA in Caenorhabditis elegans. Nature 1998 Feb 19;391(6669):806-811.
(14) Hall IM, Shankaranarayana GD, Noma K, Ayoub N, Cohen A, Grewal SI. Establishment and maintenance of a heterochromatin domain. Science 2002 Sep 27;297(5590):2232-2237.
(15) Broverman SA, Meneely PM. Meiotic mutants that cause a polar decrease in recombination on the X chromosome in Caenorhabditis elegans. Genetics 1994 Jan;136(1):119-127.
(16) Lin R. A gain-of-function mutation in oma-1, a C. elegans gene required for oocyte maturation, results in delayed degradation of maternal proteins and embryonic lethality. Dev Biol 2003 Jun 1;258(1):226-239.
(17) Austin J, Kimble J. glp-1 is required in the germ line for regulation of the decision between mitosis and meiosis in C. elegans. Cell 1987 Nov 20;51(4):589-599.
(18) Han T, Manoharan AP, Harkins TT, Bouffard P, Fitzpatrick C, Chu DS, et al. 26G endo-siRNAs regulate spermatogenic and zygotic gene expression in Caenorhabditis elegans. Proc Natl Acad Sci U S A 2009 Nov 3;106(44):18674-18679.

(19) Gu SG, Pak J, Guang S, Maniar JM, Kennedy S, Fire A. Amplification of siRNA in Caenorhabditis elegans generates a transgenerational sequence-targeted histone H3 lysine 9 methylation footprint. Nat Genet 2012 Jan 8.
(20) Berezikov E, Bargmann CI, Plasterk RH. Homologous gene targeting in Caenorhabditis elegans by biolistic transformation. Nucleic Acids Res 2004 Feb 24;32(4):e40.
(21) Ward S, Roberts TM, Strome S, Pavalko FM, Hogan E. Monoclonal antibodies that recognize a polypeptide antigenic determinant shared by multiple Caenorhabditis elegans sperm-specific proteins. J Cell Biol 1986 May;102(5):1778-1786.
(22) Grant B, Hirsh D. Receptor-mediated endocytosis in the Caenorhabditis elegans oocyte. Mol Biol Cell 1999 Dec;10(12):4311-4326.